5.1 Basic Information

Crack growth is a result of cyclic loading due to gusts and maneuvers (fatigue cracking), or of the combined action of sustained loading and environment (stress-corrosion cracking), or both. The most common crack growth mechanisms are fatigue crack growth and environment-assisted (corrosion) fatigue crack growth. Certain aircraft parts, especially high-strength forgings, may be liable to stress-corrosion cracking. Since there is a design threshold for stress corrosion, proper detail design and proper material selection can minimize or prevent stress corrosion. Fatigue cracking is difficult to prevent, but it can be controlled.

To predict crack growth behavior such as illustrated in Figure 5.1.1, the following information must be available:

- The stress-intensity factor, described as a function of crack size, for the relevant structural and crack geometry;
- The stress (load) – time history, described for the structural location component or structure under consideration;
- The baseline crack growth properties (constant amplitude crack growth rate data), described as a function of the stress intensity factor, for the material and for the relevant environment;
- A damage integration routine that integrates the crack growth rate to produce a crack growth curve, and uses the proper stress-time history, the proper stress intensity formulation, and an appropriate integration rule.

This section provides guidelines to arrive at crack growth estimates, and points out where deficiencies in knowledge and analysis methods lead to inaccuracies.

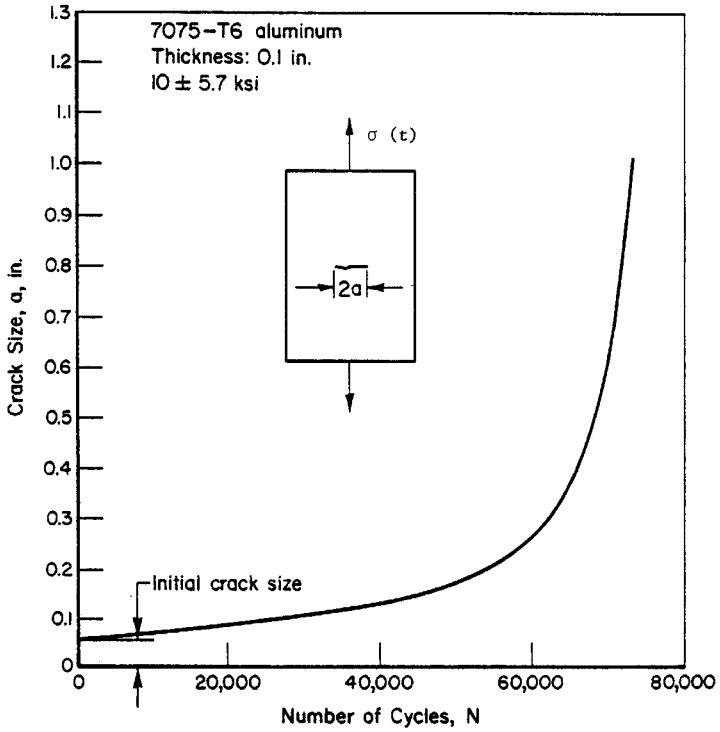

Figure 5.1.1. Typical Crack Growth-life Curve

5.1.1 Fatigue-Crack Growth and Stress-Intensity

Consider the constant-amplitude fatigue loading shown in Figure 5.1.2a. The following parameters are defined:

σ_m – mean stress

σ_a – stress amplitude

$\Delta\sigma$ – stress range

σ_{max} – maximum stress

σ_{min} – minimum stress

R – stress ratio: $R = \dfrac{\sigma_{min}}{\sigma_{max}} = \dfrac{\sigma_m - \sigma_a}{\sigma_m + \sigma_a} = 1 - \dfrac{\Delta\sigma}{\sigma_{max}}$.

The cyclic stress can be fully characterized (apart from the frequency) by any combination of two of these parameters. The stress range, $\Delta\sigma$, and the stress ratio, R, are the two most commonly used. Note that in a constant-amplitude test each of these parameters has a constant value with respect to time.

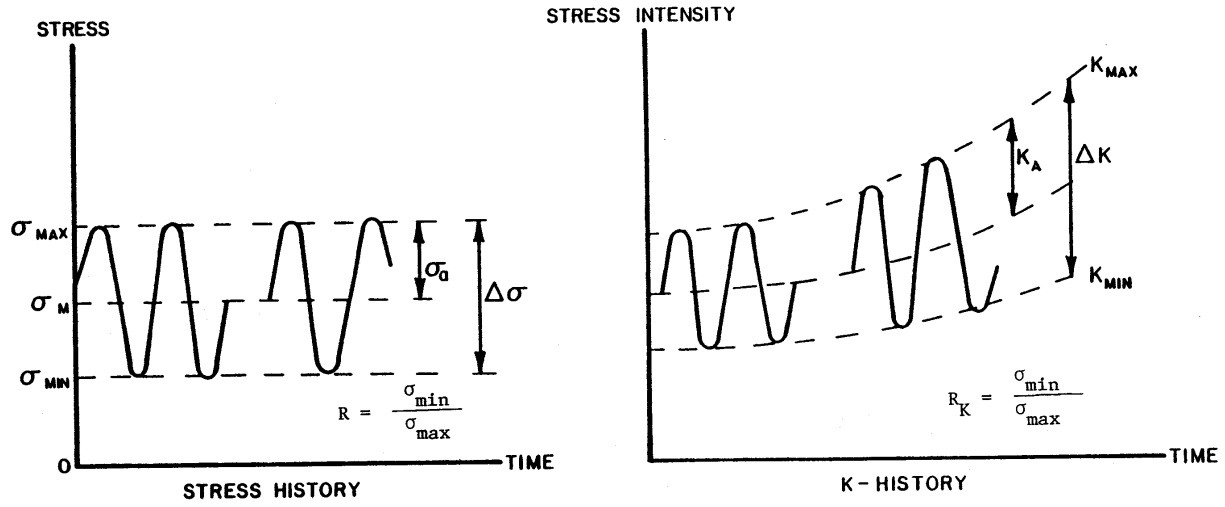

Figure 5.1.2. Definition of Terms for Fatigue Crack Growth and Stress Intensity

The stress history can be converted into a stress intensity factor history at a given crack length by multiplying the stress history by the stress intensity factor coefficient, as shown in Figure 5.1.2b. The following parameters are defined:

K_{max} – maximum stress intensity factor $= \beta\sigma_{max}\sqrt{\pi a}$

K_{min} – minimum stress intensity factor $= \beta\sigma_{min}\sqrt{\pi a}$

K_m – mean stress intensity factor $= \beta\sigma_m\sqrt{\pi a}$

K_a – amplitude of the stress intensity factor $= \beta\sigma_a\sqrt{\pi a}$

ΔK – range of the stress intensity factor $= \beta\Delta\sigma\sqrt{\pi a}$

R_K – cycle ratio: $R_K = \dfrac{K_{min}}{K_{max}}$

The above calculation schemes for stress intensity factor parameters, while being the most straightforward algebraically, have an operational quality about them. For example, it is theoretically difficult to define a negative stress intensity factor that happens if the stress becomes compressive. In this case, the crack closes and the crack tip stress field loses its singularity character; thus, the stress intensity factor ceases to have meaning. The operational quality of the negative stress intensity factors calculated for compressive stress situations has been given a lot of consideration by the aerospace industry and by ASTM, specifically its subcommittee on sub-critical crack growth (ASTM E24.04). ASTM has chosen to provide the following definitions when the minimum stress (σ_{min}) is less than zero:

$K_{min} = 0$ if $\sigma_{min} < 0$ $\qquad\qquad$ $\Delta K = K_{max}$ if $\sigma_{min} < 0$

The reader should be aware of the ASTM definition of ΔK because that convention is used in the Damage Tolerant Design (Data) Handbook [1994] for the presentation of crack growth rate data when part of the fatigue cycle is compressive, i.e., when $\sigma_{min} < 0$ ($R < 0$). The algebraic definition of ΔK is used in the current version of MIL-HDBK-5. Before negative stress ratio ($R < 0$) data are used, it is important to establish the operational definition of ΔK. The reader should note that the behavior of the material under negative stress ratio conditions is itself independent of the operational definition of ΔK.

In the elastic case, the stress-intensity factor alone is sufficient to describe the stress field at the tip of a crack. When the plastic zone at the crack tip is small compared with the crack size, the stress-intensity factor gives a good indication of the stress environment of the crack tip. Two different cracks that have the same stress environment (equal stress-intensity factors) will behave in the same manner and show the same rate of growth.

Since two parameters are required to characterize the fatigue cycle, two parameters are required to characterize crack growth rate behavior. The crack growth rate per cycle, *da/dN*, can be generally described with functional relation of the type:

$$\frac{da}{dN} = f(\Delta K, R) \quad or = g(K_{max}, R) \qquad (5.1.1)$$

where a is the crack length, N is the number of cycles, and R is the stress ratio associated with the stress cycle.

EXAMPLE 5.1.1 Meaning of *da/dN* Equation

For a wide center crack panel subjected to constant amplitude loading conditions, Equation 5.1.1 implies that the crack growth rate of a 2-inch long crack subjected to a remote loading of $\Delta\sigma = 10$ ksi for $R = 0$ will be identical to the rate of growth of a 0.5-inch long crack subjected to a remote loading of $\Delta\sigma = 20$ ksi for $R = 0$. The rates for the two different crack length - loading conditions will be the same because the stress-intensity factor range (ΔK) and the stress ratio (R) are the same in both cases.

Typically, fatigue crack growth rate data is described using plots of *da/dN* versus ΔK on double-logarithmic scale graph paper. Figure 5.1.3 presents fatigue crack growth rate data for 7075 aluminum in the graphical format that is used in the Damage Tolerant Design (Data) Handbook [1994]. Figures 5.1.4 and 5.1.5 describe example composite *da/dN* data plots for 7075 aluminum as a function of ΔK (algebraic definition) for different stress ratio (R) values [MIL-HDBK-5H, 1998]. Both Figures 5.1.4 and 5.1.5 provide mean trend curves that represent the function $f(\Delta K, R)$ in Equation 5.1.1. On the basis of these figures, it can be seen that $f(\Delta K, R)$ is not a simple function. Figure 5.1.6 is a schematic illustration of fatigue crack growth rate behavior from the threshold region (below 10^{-8} inch/cycle) to the onset of rapid cracking in the fracture toughness region (above 10^{-3} inch/cycle). As can be seen from Figures 5.1.3 - 5.1.6, the behavior exhibits a sigmoidial shape suggesting that there might be asymptotes at the two extreme regions.

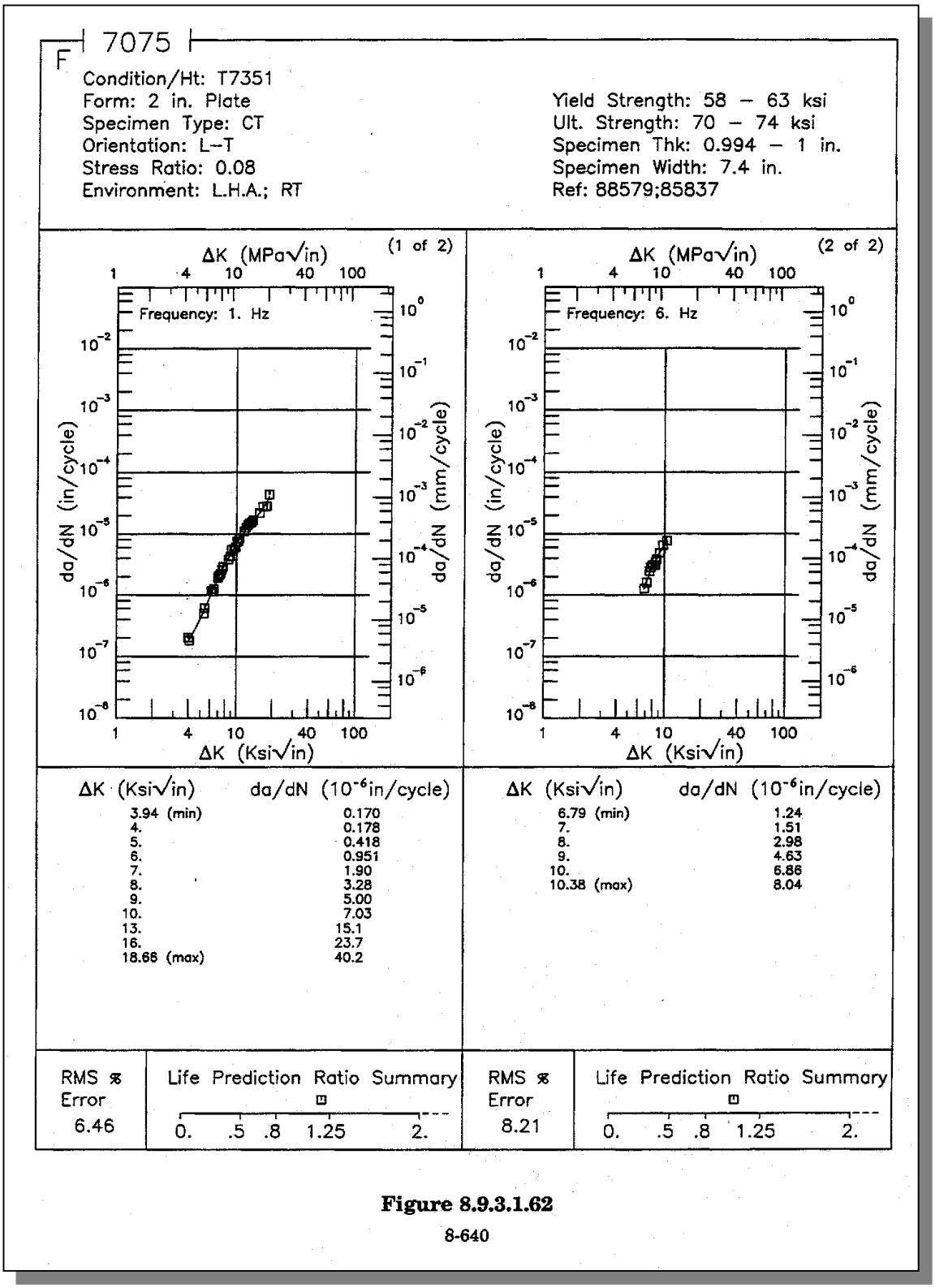

Figure 8.9.3.1.62

8-640

Figure 5.1.3. Fatigue Crack Growth Rate Data Presentation Format Used in the Damage Tolerant Design (Data) Handbook [1994]. Data Presented for Two Stress Ratios for 7057-T7351 Aluminum Alloy

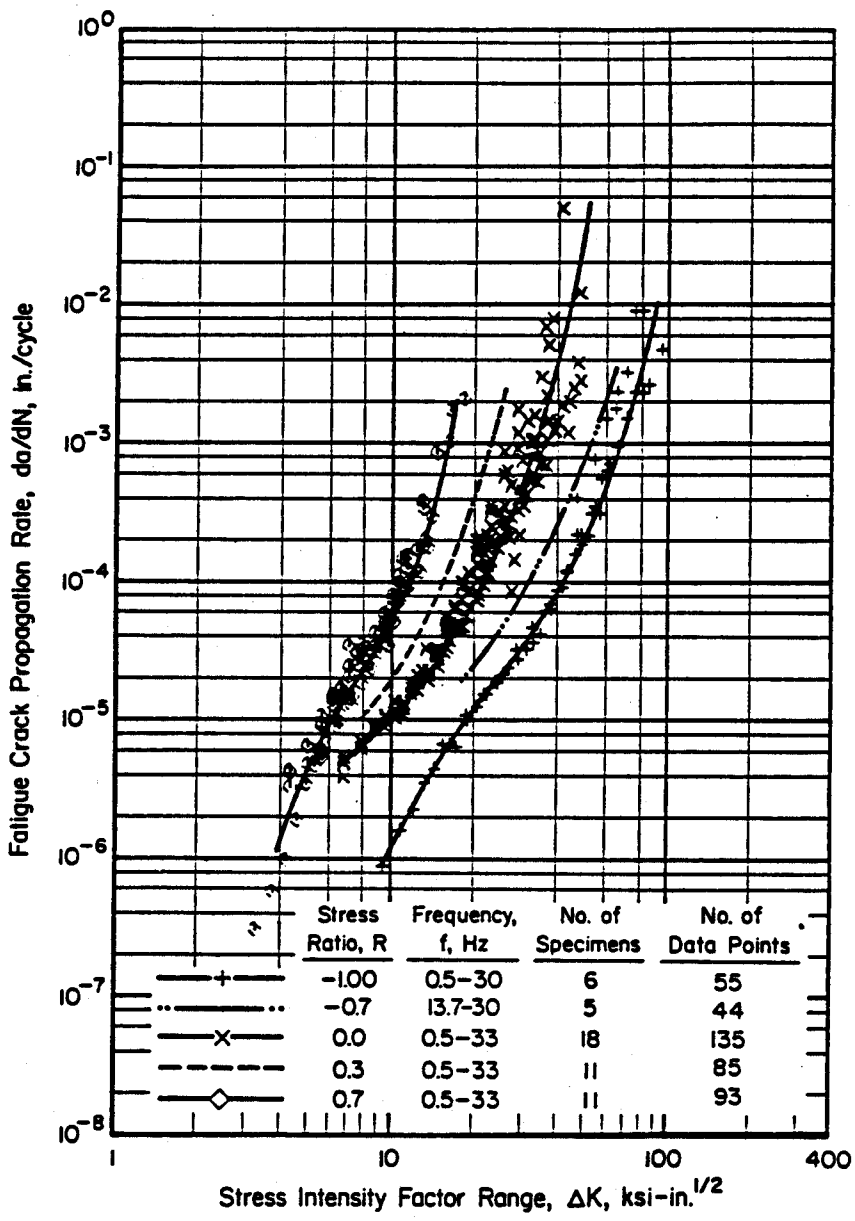

Figure 5.1.4. Sample Fatigue Crack Growth Rate Data for 7075-T6 Aluminum Alloy Sheet From MIL-HDBK-5H [1998]

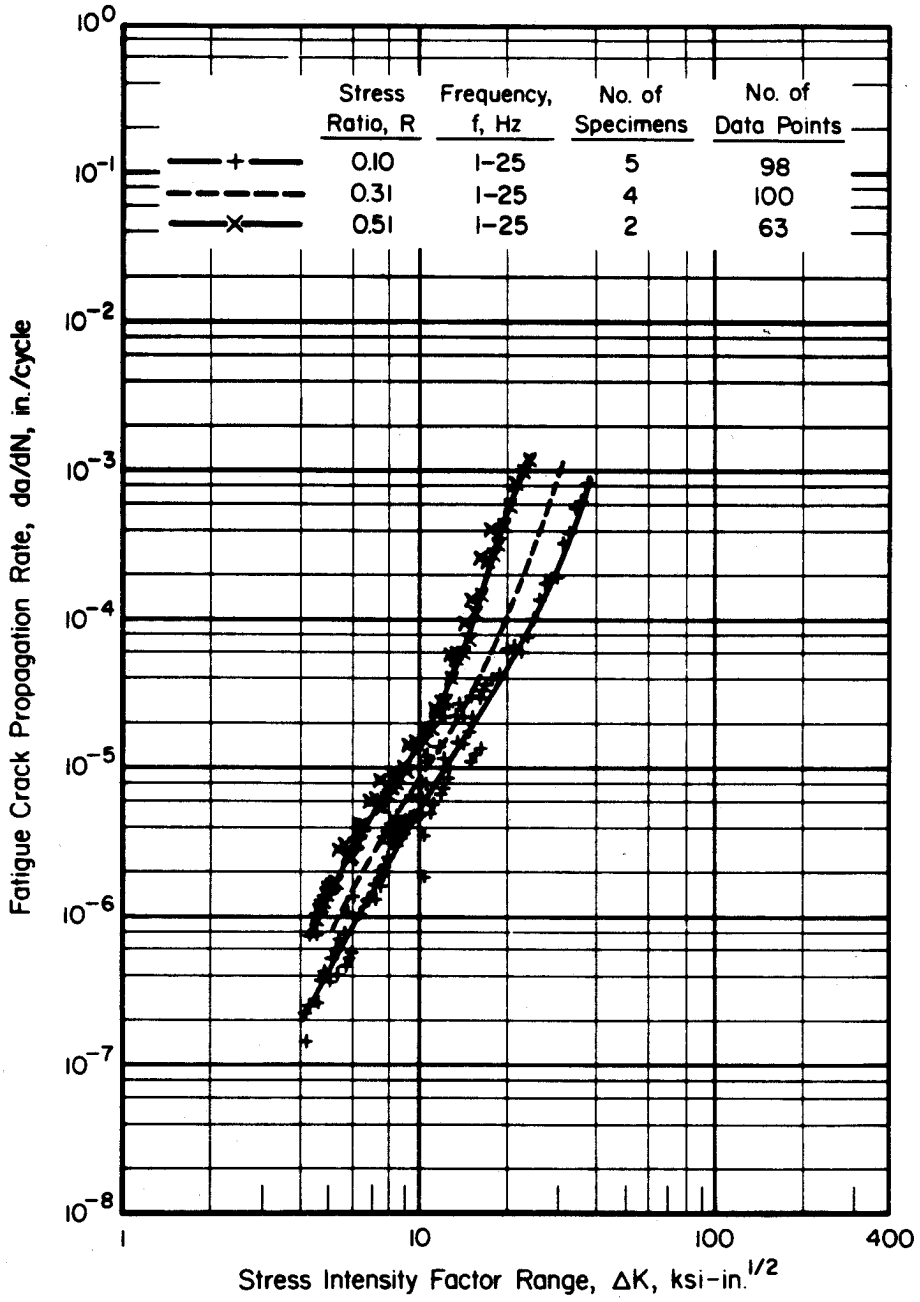

Figure 5.1.5. Sample Fatigue Crack Growth Rate Data for 7075-T7351 Aluminum Alloy Plate From MIL-HDBK-5H [1998]

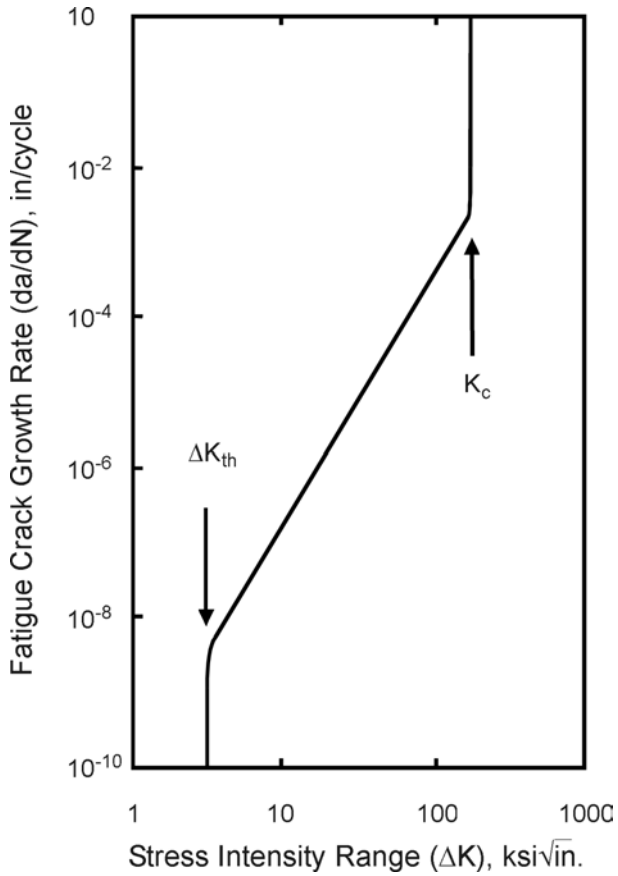

Figure 5.1.6. Schematic of Fatigue Crack Growth Rate Behavior

5.1.2 Fatigue Crack-Growth Rate (FCGR) Descriptions

Many descriptions of the function *f(ΔK, R)* in Equation 5.1.1 have been proposed. In the early literature [Pelloux, 1970; Erdogan, 1967; Toor, 1973; Gallagher, 1974], most of the descriptions were either based on physical models of the crack growth process (referred to as "laws") or on equations that appeared to describe the trends in the data. Currently, the fatigue crack growth rate (FCGR) descriptions are carefully selected to provide accurate mean trend descriptions of the specific data collected to support a materials evaluation or structural design. Before introducing these more accurate FCGR descriptions, the Paris power law [Paris, 1964], the Walker equation [Walker, 1970], and Forman equations [Forman, et al., 1964] will be reviewed.

The Paris power law equation was initially proposed to describe the crack growth rate behavior in the central region for specific values of stress ratio. This equation is given by the general form:

$$\frac{da}{dN} = C\Delta K^{p} \qquad (5.1.2)$$

where C and p are experimentally determined constants. Equation 5.1.2 is still extensively used to develop first order approximations of life behavior when only limited amounts of data are available. The reader is cautioned that Equation 5.1.2, as well as any other FCGR description, should not be extrapolated beyond its limits of applicability without a great deal of care and

experience. Greater life prediction errors can result from data extrapolation errors than almost all other design methodology errors combined.

The Walker equation provided one of the first simple equations that accounted for the stress ratio shift. It is a subtle modification of Equation 5.1.2 and is given by

$$\frac{da}{dN} = C\left[(1-R)^m K_{max}\right]^p \qquad (5.1.3)$$

where C, m, and p are empirical constants. The exponent m typically ranges from 0.4 to 0.6 for many materials. Because Equation 5.1.3 is a power law, it has been noted to be most useful in describing the central region of the growth rate behavior.

The Forman equation was initially proposed to describe both the central and high crack growth regions of the behavior. To account for the acceleration of the cracking rates as the stress-intensity factors levels approached critical, the Paris power law equation was divided by a factor that would reach zero when the stress-intensity factor reached a critical level. The general form of the Forman equation is:

$$\frac{da}{dN} = \frac{C\,\Delta K^p}{(1-R)K_c - \Delta K} \qquad (5.1.4)$$

where C, p, and K_c are experimentally evaluated for the given material and thickness. Equation 5.1.4 can be rearranged to yield:

$$\frac{da}{dN} = \frac{C\,(1-R)^{p-1}.K^p{}_{max}}{K_c - K_{max}} \qquad (5.1.5)$$

which shows that the equation has the capability to describe multiple stress ratio data sets.

The empirical constants in Equations 5.1.2 - 5.1.4 are typically derived using least square fitting procedures. Note that the simplicity of Equations 5.1.2 and 5.1.3 allow for a graphical fit to the data on log-log coordinate paper and the direct evaluation of the constants from the graph. The usefulness of Equations 5.1.2 - 5.1.4 comes from the ease in which their constants can be evaluated from available data, as well as the direct application of the equations to simplified life integration calculations. When considering the general expression for crack growth life (N_f)

$$N_f = \int_{a_o}^{a_f} \frac{da}{f(\Delta K, R)} \qquad (5.1.6)$$

it is seen that the function f is simple for Equations 5.1.2 - 5.1.4.

One modeling procedure that has consistently shown itself to range among the most accurate FCGR descriptions for predicting lives is the table look-up scheme . For life prediction purposes, many aircraft companies have gone to a table look-up scheme in which they describe crack growth rate as a function of ΔK for specific values of fatigue crack growth rate or vice versa, i.e., da/dN is described for specific values of ΔK.

Table 5.1.1 summarizes the mean trend FCGR behavior of the 2219-T851 aluminum alloy employed by the ASTM Task Group E24.04.04. Within the main body of Table 5.1.1, da/dN are presented as a function of pre-chosen ΔK levels for specific levels of stress ratio (or environment, etc.). In the rows directly above and directly below the main body of the table, the data extreme

values are defined. In the bottom rows of the table, statistical summaries that define the accuracy of the mean trend (tabular) description relative to the FCGR data and with respect to life prediction (life prediction ratios based on original a vs. N data). The RMSPE (root mean square percentage error) is a statistic that measures the deviation of fatigue crack growth rate data from the table; and, it is somewhat akin to the coefficient of (life) variation.

The mean trend data presented in the Damage Tolerant Design (Data) Handbook [1994] can be directly utilized with table look-up algorithms in crack growth life prediction computer codes. These data might also be utilized with least square fitting procedures to generate wider ranging predictive schemes that account for the effects of stress ratio, frequency, environment, temperature, and other controlling conditions.

The Damage Tolerant Design (Data) Handbook provides crack-growth data for a variety of materials. The data are presented in the form of graphs and tables, as shown in Figure 5.1.3. Multiple parameter equation fitting should not be attempted if only limited sets of data are available. In case limited data sets have to be used, a comparison should be made with similar alloys for which complete data are available, and curves may be fitted through the limited data sets on the basis of this comparison.

Table 5.1.1. Example Fatigue Crack Growth Rate Table (2219-T851 Aluminum)

$\Delta K\left(ksi\sqrt{in}\right)$			$da/dN \times 10^6$ **inches/cycle**				
			R_1=-1.0	**R_2=0.1**	**R_3=0.3**	**R_4=0.6**	**R_5=0.8**
ΔK_{min} at:	R_1	1.09	0.00730				
	R_2	2.55		0.00336			
	R_3	2.11			0.00369		
	R_4	1.38				0.00351	
	R_5	1.17					0.00112
		1.3	0.0167				0.00429
		1.6	0.0351			0.0176	0.0251
		2.0	0.0676			0.0569	0.0689
		2.5	0.127		0.0451	0.0911	0.128
		3.0	0.216	0.0166	0.152	0.139	0.228
		3.5	0.336	0.0639	0.246	0.218	0.431
		4.0	0.488	0.171	0.355	0.339	0.809
		5.0	0.884	0.566	0.691	0.753	2.60
		6.0	1.37	1.14	1.30	1.46	7.83
		7.0	1.91	1.93	2.28	2.50	46.3
		8.0	2.47	3.09	3.60	3.95	
		9.0	3.08	4.78	5.14	6.07	
		10.0	3.80	7.04	6.86	9.38	
		13.0	7.16	17.0	14.4	38.4	
		16.0	13.2	36.2	30.9		
		20.0	28.3	126.0			
ΔK_{max} at:	R_1	20.7	32.0				
	R_2	24.7		887.0			
	R_3	19.3			81.3		
	R_4	15.8				146.0	
	R_5	7.01					47.4
RMSPE			2.2	80.4	8.6	6.4	6.1
Life prediction ratio summary							
0.0-0.5			1				
0.5-0.8				1			
0.8-1.25				3	1	2	2
1.25-2.0							
>2.0							

ASTM Task Group E24.04.04 on FCGR descriptions conducted two analytical round robin investigations of the utility of various FCGR descriptions that describe crack growth behavior [Miller, et al., 1981; Mueller, et al., 1981]. These round robin investigations have clearly demonstrated that FCGR descriptions which are classified as "good" from a life analysis standpoint must adequately represent the mean trend of the FCGR data. Figure 5.1.7 outlines a general procedure whereby the FCGR behavior is first described by least square regression analysis (Figure 5.1.7a) and then the regression equation, in conjunction with the stress-intensity factor analysis for the test geometry, is used in integral form to obtain an estimate of the fatigue crack growth life N_f (Figure 5.1.7b). In Figure 5.1.7a, the mean trend behavior is described along with bounds on the regression equation. Those descriptions which fail to model the mean trend of the FCGR data, either because they are preconceived to have a specific form (sinh, power law, Forman, etc.) or due to a lack of care in performing the regression analysis, lead to life prediction errors that are biased or exhibit significant scatter.

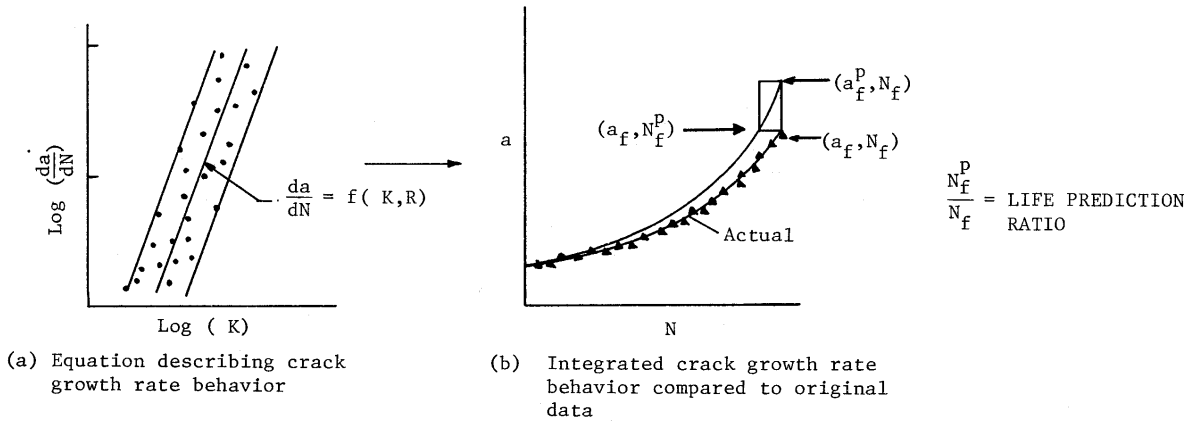

Figure 5.1.7. Description of FCGR Data Fitting and the Comparison of Predicted to Actual Behaviors

To support the first round robin, FCGR data from compact and center crack test geometries fabricated from 0.25 inch thick 2219-T851 aluminum alloy were supplied to the participants. The tests were conducted between threshold and fracture toughness levels for five separate stress ratios (-1, 0.1, 0.3, 0.5, and 0.8). A number of individuals from government, industry, and academia participated in the round robin (see Table 5.1.2) and chose to evaluate the ten (10) descriptions defined in Table 5.1.3. Each participant was given FCGR data and asked to describe the mean trend of the behavior using equations or other procedures. The participants then integrated their mean trend analysis to establish predicted life values. They were each given the initial and final crack sizes as well as the loading conditions for these life predictions of center crack specimens and compact specimens.

Table 5.1.2. Active Participants and their Organizations for Round Robin Investigation [Miller, et al., 1981]

Name	Affiliation
C.G. Annis F.K. Haake	Pratt & Whitney Aircraft
J. Fitzgerald	Northrop Corporation
J.P. Gallagher* M.S. Miller	University of Dayton Research Institute
S.J. Hudak, Jr. A. Saxena	Westinghouse R & D Center
J.M. Krafft	Naval Research Laboratory
D.E. Macha	Air Force Materials Laboratory
L. Mueller+	Alcoa Laboratories
B. Mukherjee M.L. Vanderglas	Ontario Hydro
J.C. Newman	NASA Langley Research Center

*Chairman, ASTM Task Group E24.04.04 on FCGR Descriptions (1975 - 80)
+Chairman, ASTM Task Group E24.04.04 on FCGR Descriptions (1980 - 83)

One of the procedures utilized to evaluate the ten descriptions was to summarize the sixteen (16) life prediction ratios (life predicted divided by life measured, N^P_f/N_f, see Figure 5.1.7b) associated with each description. The means and standard deviations for the life prediction ratios associated with each participant/FCGR description is presented in Table 5.1.4.

Table 5.1.3. FCGR Descriptions for Round Robin Investigation

Participant/FCGR Description No.	Form
(1)	$\frac{da}{dN} = C_1 \overline{\Delta K}^{C_2}$
(2)	$\frac{da}{dN} = P_1 \frac{(\Delta K - \Delta K_t)^{P_2}}{(\Delta K_c - \Delta K)^{P_3}}$
(3)	$\frac{1}{da/dN} = \frac{A_1}{(\Delta K)^{n_1}} + A_2 \left[\frac{1}{(\Delta K)^{n_2}} - C' \right]$
(4)	$\frac{da}{dN} = C(K_{\max})^m \left[(K_{\max} + K_e)(1 - R_{eff}) + {}^*K \right]^2$
(5)	$\log_{10}\left(\frac{da}{dN} \right) = P_1 \exp(P_2 x) + P_3 \exp(P_4 x) + P_5$
$(6)^+$	$\frac{da}{dN} =_{10} \{C_1 sihn[C_2(\log \Delta K + C_3)] + C_4\}$
$(7)^+$	$\frac{da}{dN} =_{10} \{C_1 sihn[C_2(\log \Delta K + C_3)] + C_4\}$
(8)	$\frac{da}{dN} = e + (v - e) \left[-\ln\left(1 - \frac{\Delta K}{K_b} \right) \right]^{1/k}$
(9)	Tensile ligament instability model
(10)	Table lookup procedure

+ The hyperbolic sine model is listed twice because two separate organizations chose to evaluate this description.

The life prediction ratio (LPR) numbers in Table 5.1.3 can be interpreted by comparing the mean LPR to 1.0 and the standard deviation to 0.0. A mean LPR less than 1.0 implies a conservative prediction. A further interpretation of the results of the round-robin are also presented in Table 5.1.3 with the percentage of life prediction ratios that fall within the ranges of 0.80 and 1.20 and of 0.90 and 1.10. Note that five descriptions were able to achieve LPR numbers between 0.80 and 1.20 for at least 80 percent of the number of predictions made.

Table 5.1.4. Comparison of FCGR Descriptions

Participant/FCGR Description No.	Mean	Standard Deviation	Percent of All Predictions Within:	
			± 20% of 1.0	± 10% of 1.0
1	0.95	0.27	53.3	20.0
2	0.72	0.16	33.3	20.0
3	1.00	0.27	86.7	26.7
4	0.76	0.15	38.5	15.4
5	0.96	0.12	100.0	73.3
6	0.97	0.24	73.3	53.3
7	2.32	5.81	80.0	66.7
8	0.99	0.10	89.5	57.9
9	1.05	0.32	31.3	18.8
10	0.96	0.12	100.0	80.0

5.1.3 Factors Affecting Crack Growth

Unlike tensile strength and yield strength, fatigue crack growth rate (FCGR) behavior is not a consistent material characteristic. The FCGR is influenced by many uncontrollable factors. As a result, a certain amount of scatter occurs. Therefore, crack growth predictions should be based on factors relevant to the conditions in service.

Among the many factors that affect crack propagation, the following should be taken into consideration for crack growth properties:

Material production:

- Type of product (plate, extrusion, forging)
- Heat treatment
- Orientation with respect to grain direction
- Manufacturer and batch
- Thickness

Environmental conditions:

- Environment
- Temperature
- Frequency

No attempt will be made to illustrate the effects of all these factors with data, particularly because some factors have largely different (and sometimes opposite) effects on different materials. Rather, some general trends will be briefly mentioned.

Several factors pertaining to the material production affect crack growth. The crack propagation characteristics for a particular alloy differ for plates, extrusions, and forgings. The latter may exhibit large anisotropy, which may have to be considered in the growth of surface flaws and corner cracks, which grow simultaneously in two perpendicular directions. Closely related to this are other processing variables, particularly the heat treatment.

An alloy of nominally the same composition but produced by different manufacturers may have quite different crack propagation properties [Schijv & DeRijk, 1966]. This is illustrated in Figure 5.1.8. The differences are associated with slight variations in composition, inclusion content, heat treatment (precipitates), and cold work. Similar variations in crack growth occur for different batches of the same alloy produced by the same manufacturer. Data presented in Figure 5.1.9 show that growth rates can vary with sheet thickness [Broek, 1963; Broek, 1966; Raithby & Bibb, et al., 1961; Donaldson & Anderson, 1960; Smith, et al., 1968].

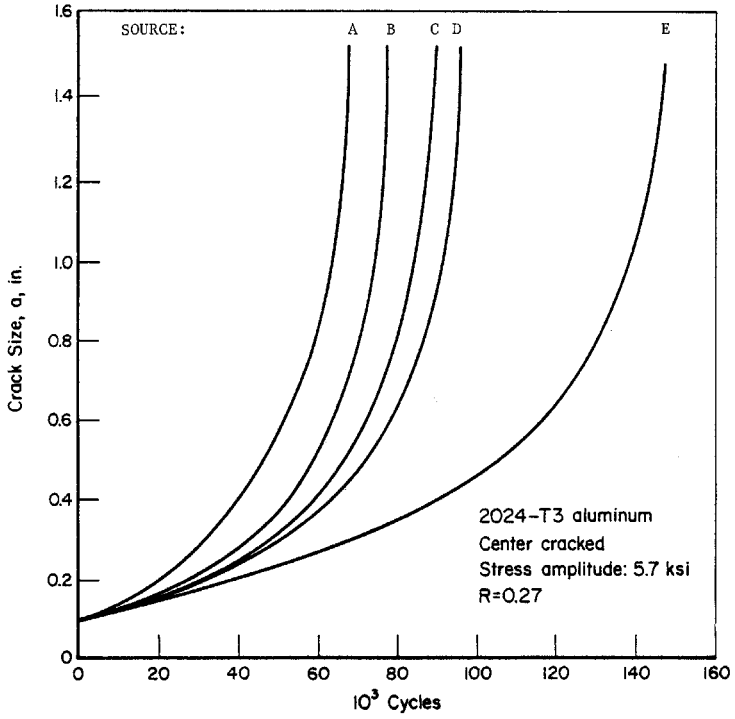

Figure 5.1.8. Possible Variation of Crack Growth in Materials from Different Sources [Schijve & DeRijk, 1966]

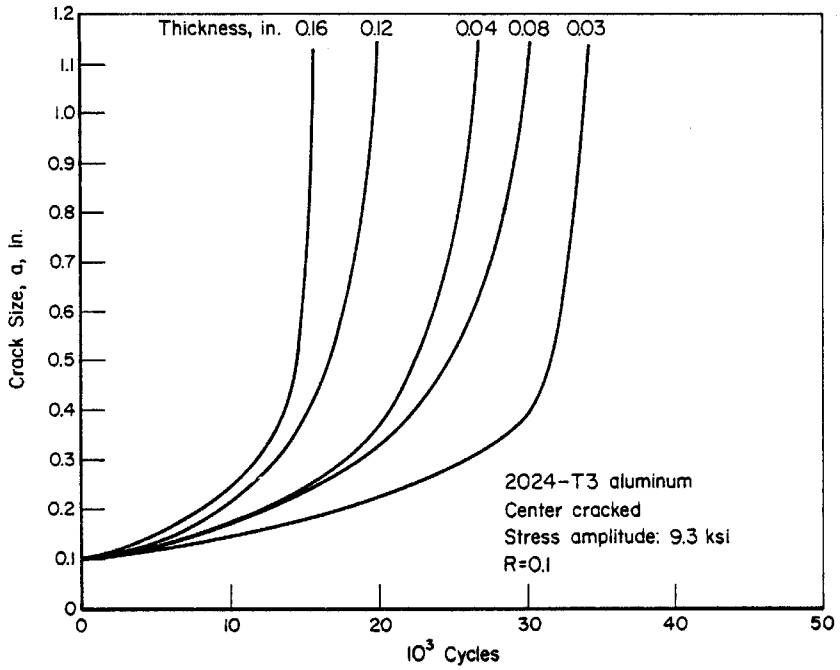

Figure 5.1.9. Example of Effect of Thickness on Crack Growth [Broek, 1963]

In view of the factors that influence crack growth properties, predictions of crack growth should be based on material data that pertain to the product form. Spot checks may be necessary to account for variability in heats and/or manufacturer.

The factors pertaining to environmental conditions are associated with the environmental circumstances. A lightly corrosive environment (humid air) gives rise to higher crack growth rates than a dry environment [Hartman, 1965; Piper, et al., 1968; Bradshaw & Wheeler, 1969; Dahlberg, 1965; Meyn, 1971; Meyn, 1968; Achter, 1967; Wei, 1970; Hartman & Schijve, 1970; Shih & Wei, 1974]. The effect is illustrated in Figure 5.1.10. Although opinions differ in explaining the environmental effect, there is concurrence that the principal factor is corrosive action, which is time and temperature dependent. The effect of cyclic frequency [Piper, et al., 1968; Meyn, 1971; Hartman & Schijve, 1970; Schijve & Brock, 1961] is related to the environmental effect, with slower cyclic frequencies usually associated with accelerated fatigue crack growth rates.

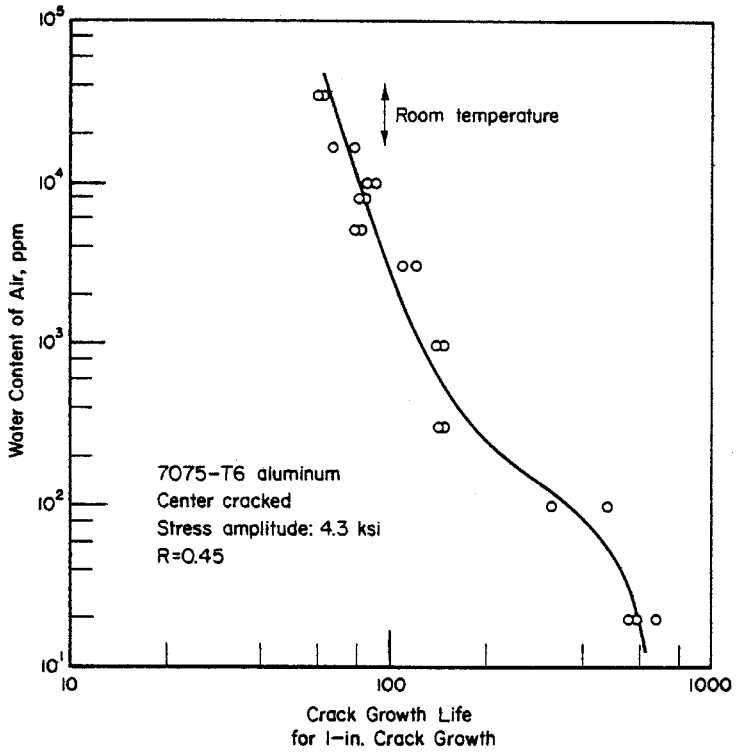

Figure 5.1.10. Effect of Humidity on Fatigue Crack Propagation [Hartman, 1965]

At low temperatures, the reaction kinetics are slower and the air contains less water vapor. This may reduce crack propagation rates in certain alloys [Broek, 1972; Tobler, et al., 1974]. Figure 5.1.11 shows the influence of low temperature on crack growth for 7075-T6 alloy compared with growth at normal temperatures [Broek, 1972]. Temperatures higher than ambient may increase crack growth rates [Schijve & DeRijk, 1963; Lachnaud, 1965].

In view of the effect of environment on crack growth, the data used for life predictions should represent the effect of the expected environment and temperature.

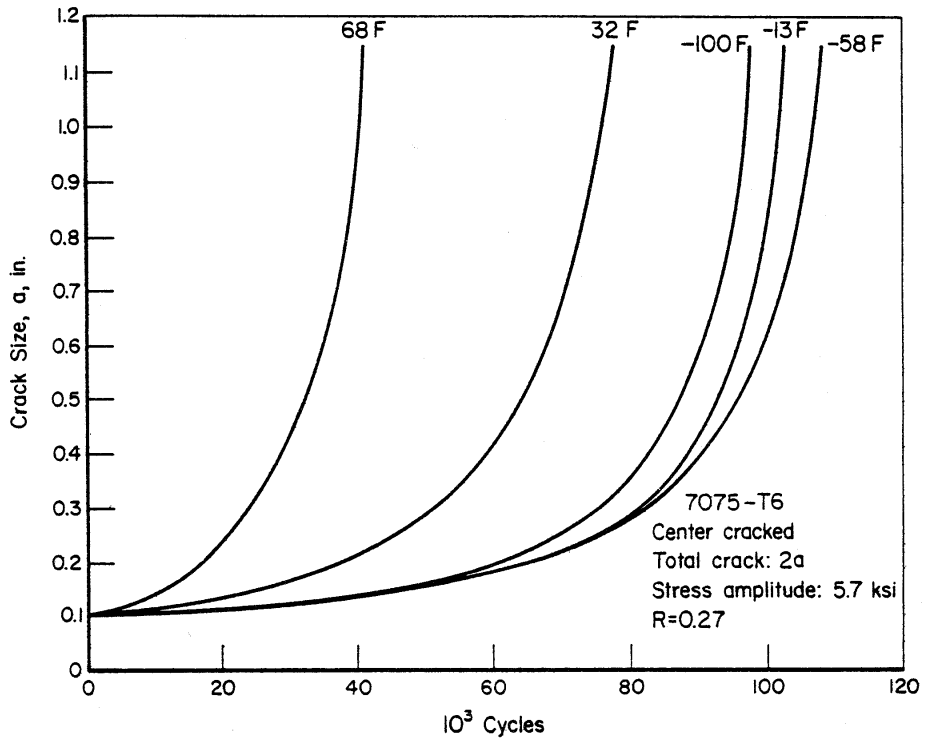

Figure 5.1.11. Example of Temperature Effect on Crack Growth [Broek, 1972]

5.1.4 Use of Data and Data Scatter

Fatigue-crack-propagation data for a variety of materials can be found in data handbooks. In many cases, because of unique material condition, thickness and environment, the data for a particular application will have to be generated in the manner prescribed by Section 7.

As indicated by the results presented in the previous section, accurate mean trend FCGR descriptions result in accurate fatigue crack life descriptions. People have worried in the past about trying to account for the substantial amount of scatter that exists in the crack growth rate data. The amount of crack growth between crack measurements and the accuracy of this incremental crack growth measurement determines a large part of the scatter. Another inherent reason for data scatter is due to the differentiation techniques that one uses to reduce the data.

Figure 5.1.12a shows a hypothetical example of the crack growth-life behavior observed in a single laboratory test; Figure 5.1.12b represents the FCGR data derived from this test. An asterisk in Figures 5.1.12a and b indicates outlying data points. The mean trend curves faired through the data are directly related to each other; the integral of the curve in Figure 5.1.12b gives the curve in Figure 5.1.12a for the test conditions. If more tests are run and all the data compiled, the plot is as shown in Figure 5.1.12c; each test might have a few outlying data points, but the compilation has many outlying points. When all data points, including the outliers, are plotted, the data exhibit a wide scatter-band, noted as the apparent scatter-band, shown in Figure 5.1.12c. However, as previously seen from Figures 5.1.12a and b, the outlier points did not significantly affect the crack growth curve or the mean trend FCGR curve. When considered collectively, the outlying data points in Figure 5.1.12c can be misleading since they do not represent the mean trend behavior of any specimen. If the wide scatter-band were considered for

a crack growth prediction, the upper bound would predict a consistent high growth rate for each crack size (whereas it happened only incidentally as shown in Figure 5.1.12a). As a result, the diagram would reflect a large apparent scatter in crack growth lives (Figure 5.1.12d), whereas the real scatter in crack growth lives is much smaller.

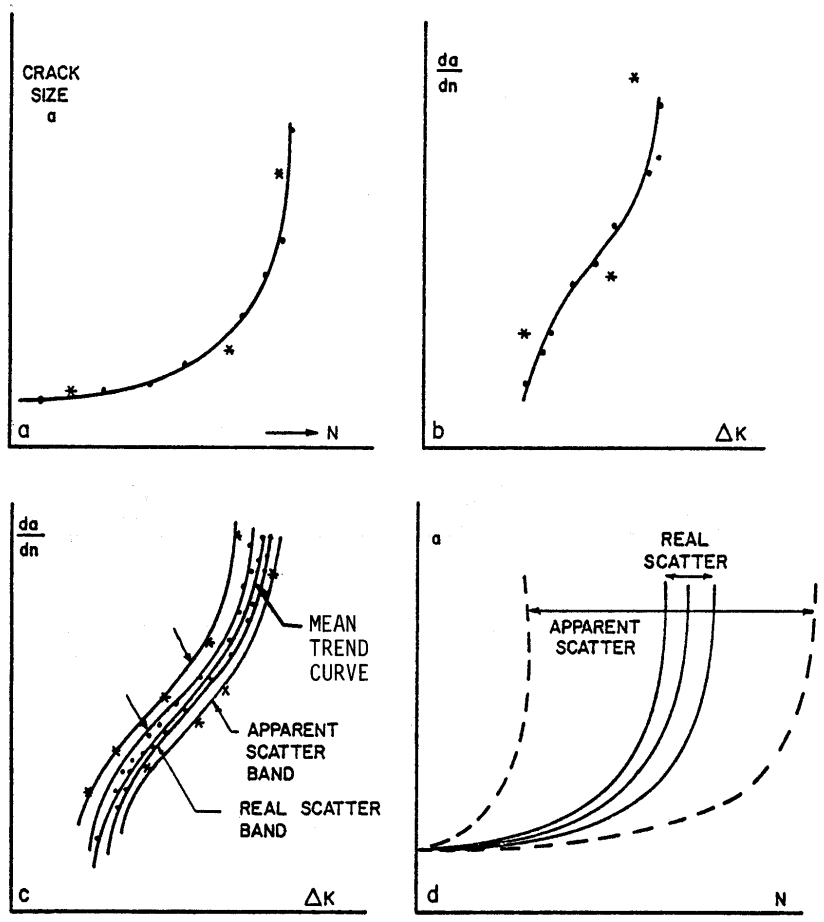

Figure 5.1.12. Crack Growth Data Scatter for Identical Conditions

As indicated by the above remarks, worrying about the random (within specimen) scatter in fatigue crack growth rates is really not that important from a life estimation standpoint. What has been found from analyses of multiple specimen data sets is that the width of the scatter-bands associated with specimen to specimen mean trend variations in FCGR is closely related to the variability in crack growth-life behavior. The scatter-band associated with specimen to specimen variations is identified in Figures 5.1.12c and d as the real scatter-band since it focuses on the variability in crack growth-life behavior.

The coefficient in variation of crack growth lives is sometimes similar in magnitude to the root mean square (percentage) error associated with fatigue crack growth rate modeling. When conservative estimates in crack growth lives are desired, the upper bound of the real scatter-band (identified in Figure 5.1.12c) determined on the basis of four or more specimens should be used.

5.1.5 Stress-Corrosion Cracking and Stress Intensity

Many engineering materials exhibit some cracking behavior under sustained loading in the presence of an environment (thermal and/or chemical). The type of cracking behavior for many chemical environments is referred to as stress-corrosion cracking behavior. The mechanism for this attack process has been attributed to the chemical reactions that take place at the crack tip and to diffusion of reactive species (particularly hydrogen) into the high stressed region ahead of the crack. The cracking process has been noted to be a function of time and it is highly dependent on the environment, the material, and the applied stress (or stress-intensity factor) level.

For a given material-environment interaction, the stress-corrosion-cracking rate has been noted to be governed by the stress-intensity factor. Similar specimens with the same size of initial crack but loaded at different levels (different initial K values) show different times to failure [Brown, 1968; Sullivan, 1972; Chu, 1972], as shown in Figure 5.1.13. A specimen initially loaded to K_{Ic} fails immediately. The level below which cracks are not observed to grow is the threshold level that is denoted as K_{Iscc}.

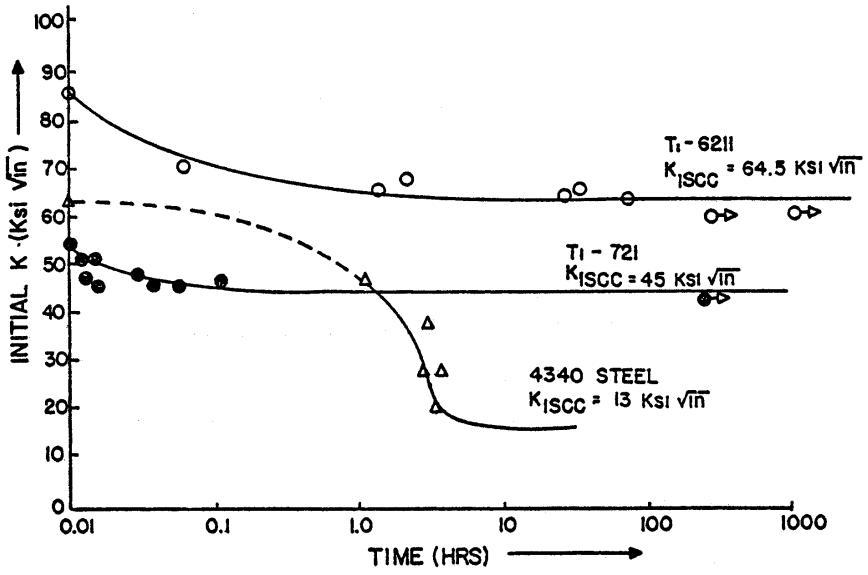

Figure 5.1.13. Stress Corrosion Cracking Data [Brown, 1968]

If the load is kept constant during the stress-corrosion-cracking process, the stress-intensity factor will gradually increase due to the growing crack. As a result, the crack-growth rate per unit of time (da/dt) increases according to

$$\frac{da}{dt} = f(K) \qquad (5.1.7)$$

When the crack has grown to a size so that K becomes equal to $K_{Ic,}$ the specimen fails. This is shown schematically in Figure 5.1.14. In typical tests, specimens may be loaded to various initial K's such as K_1, K_2, and K_3. The time to failure is recorded giving rise to the typical data point (t_1, K_1). During the test, K will increase, as a result of crack extension, from its initial value to K_{Ic}, when final failure occurs. The times t_2 and t_3 represent the time to failure for higher K's such as K_2 and K_3.

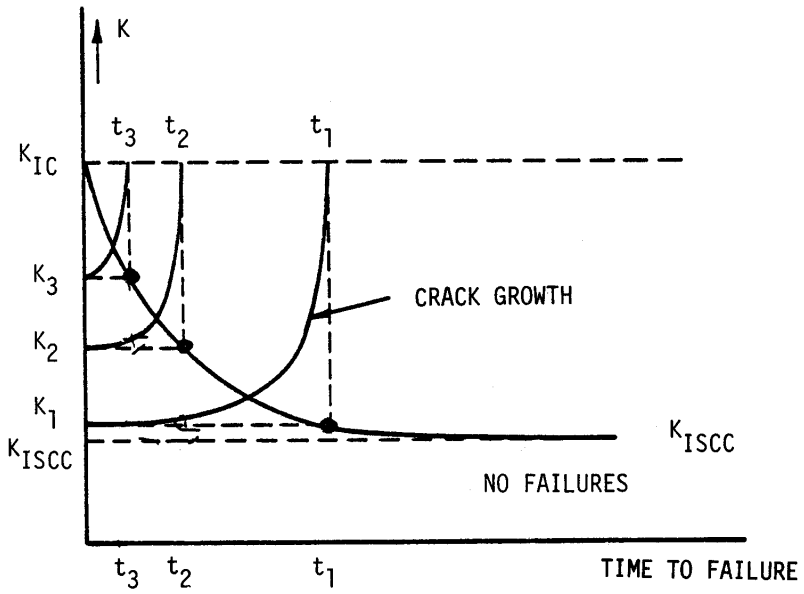

Figure 5.1.14. Stress Corrosion Cracking

The stress-corrosion threshold and the rate of growth depend on the material and the environmental conditions. Data on K_{Iscc} and *da/dt* can be found in the Damage Tolerant Design (Data) Handbook [1994] . Typical examples of K_{Iscc} and *da/dt* data presentation formats are shown in Figures 5.1.15 and 5.1.16.

TABLE 7.5.3.3

(1 of 2)

K_{Iscc} SUMMARY FOR ALUMINUM ALLOY 2024

Condition/ Heat Treat	Prod Form	Test Temp (°F)	Spec Or.	Yield Str (Ksi)	Environment	Specimen			Prod Thk (in)	Crack (in)	K_Q (Ksi√in)	K_{Iscc} (Ksi√in)	Test Time (min)	Test Date	Reference
						Thick (in)	Design	Width (in)							
T351	P	R.T.	S-L	47	3.5% NaCl	1	DCB	5	1	---	50	10	---	1969	78313
				42.4	Industrial Atm	1	CT	2	2.5	---	21.2	10	---	1973	86688
					Salt-Dichromate-Acetate	1	CT	2	2.5	---	21.2	9	---	1973	86688
					Seacoast Atm	1	CT	2	2.5	---	21.2	10	---	1973	86688
T352	F	R.T.	S-L	43.3	Seawater	0.7	DCB	1.4	6	---	27.6	23*	---	1972	82675
T851	P	R.T.	L-T	59.3	3.5% NaCl	1.25	TDCB	5	3.2	---	18.6	21.5	---	1971	84360
					Air 78% RH	1.25	TDCB	5	3.2	---	18.6	22.7	---	1971	84360
					Dist Water	1.25	TDCB	5	3.2	---	18.6	22	---	1971	84360
					JP-4 Fuel	1.25	TDCB	5	3.2	---	18.6	21.6	---	1971	84360
			S-L	61.8	Industrial Atm	1	CT	2	2.5	---	16.7	16	---	1973	86688
					Salt-Dichromate-Acetate	1	CT	2	2.5	---	16.7	15	---	1973	86688
					Seacoast Atm	1	CT	2	2.5	---	16.7	16	---	1973	86688
T852	F	R.T.	L-T	53	S.C.S.	1	DCB	5.5	3	---	34	22.1	64920	1976	RI006
						1	DCB	5.5	3	---	34	34*	61680	1976	RI006
				58	S.T.W.	1	DCB	5.5	3	---	37	22.5	76140	1976	RI006
						1	DCB	5.5	3	---	37	>23.5	76140	1976	RI006
						1	DCB	5.5	3	---	37	22.5	76140	1976	RI006

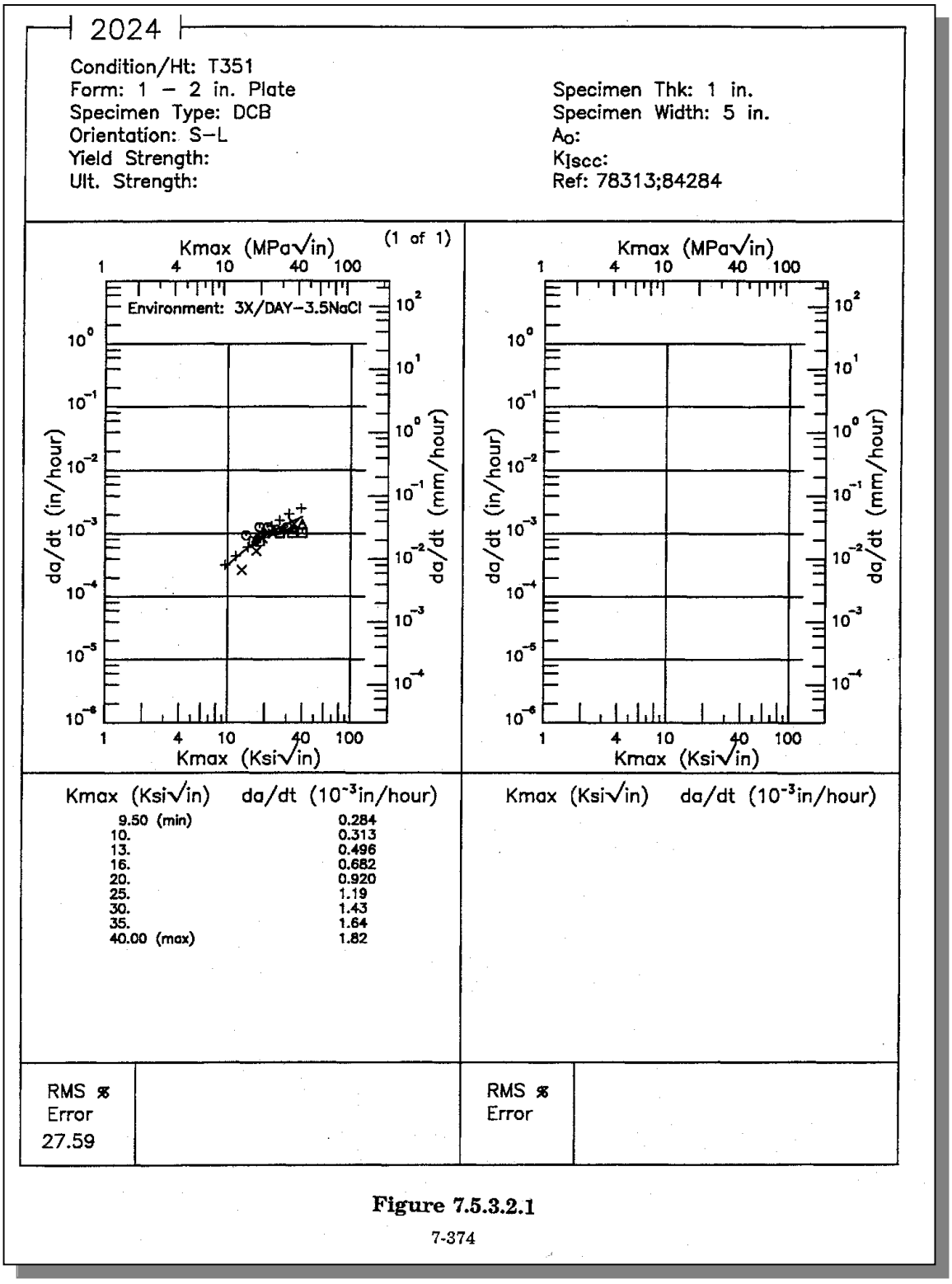

Figure 5.1.16. Stress Corrosion Cracking Rate Data for 2024-T351 Aluminum as Presented by the Damage Tolerant Design (Data) Handbook [1994]

As illustrated in Figure 5.1.17, a component with a given crack fails at a stress given by

$$\sigma_c = \frac{K_{Ic}}{\beta\sqrt{\pi a}}$$

It will exhibit stress-corrosion-crack growth when loaded to stresses in excess of

$$\sigma_{scc} = \frac{K_{Iscc}}{\beta\sqrt{\pi a}}$$

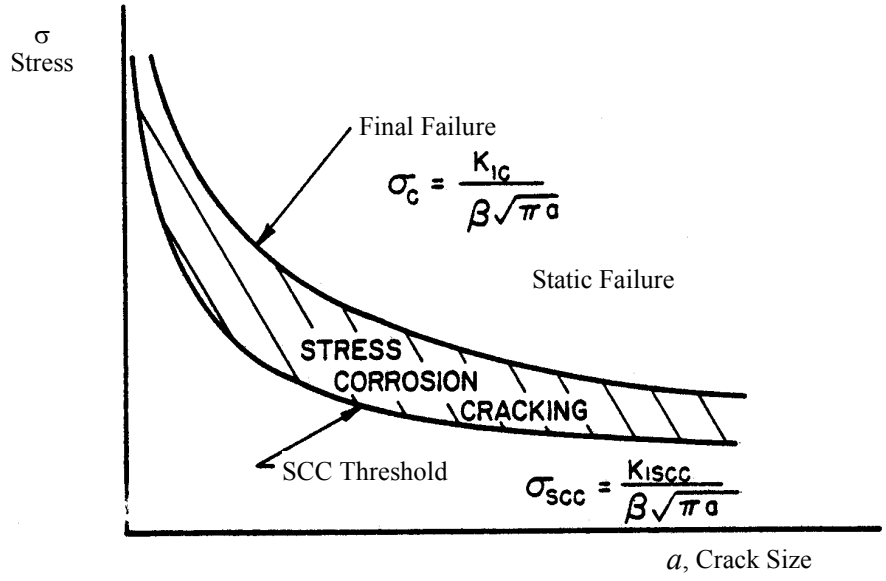

Figure 5.1.17. Stress Required for Stress Corrosion Cracking

In service, stress-corrosion cracks have been found to be predominantly a result of residual stresses and secondary stresses. Stress-corrosion failure due to primary loading seldom occur because most stress-corrosion cracks favor the short transverse direction (S-L), which is usually not the primary load direction. In many materials, the long transverse (T-L) and longitudinal (L-T) directions are not very susceptible to stress corrosion.

Prevention of stress corrosion cracking is preferred as a design policy over controlling it as is done for fatigue cracking. This means that stress-corrosion critical components must be designed to operate at a stress level lower than

$$\sigma_{scc} = \frac{K_{Iscc}}{\beta\sqrt{\pi a_i}}$$

in which a_i is the initial flaw size as specified in the Damage Tolerance Requirements of JSSG-2006. However, if stress corrosion can occur, it must be accounted for in damage tolerance analyses by using an integral form of Equation 5.1.7.

Stress-corrosion cracking may occur in fatigue-critical components. This means that in addition to growth by fatigue, cracks might show some growth due to stress corrosion. In dealing with this problem, the following should be considered:

- Stress-corrosion cracking is a phenomenon that basically occurs under a steady stress. Hence, the in-flight stationary stress level (l g) is the governing factor. Most fatigue cycles are of relatively short duration and do not contribute to stress-corrosion cracking. Moreover, the cyclic crack growth would be properly treated already on the basis of data for environment-assisted fatigue-crack growth. When stress corrosion cracking is expected, the stress corrosion cracking rate should be superimposed on the fatigue crack growth rate [Wei & Candes, 1969; Gallagher & Wei, 1972; Dill & Saff, 1978; Saff, 1980].
- Stress-corrosion cracking is generally confined to forgings, heavy extrusions, and other heavy sections, made of susceptible materials. Thus, the problem is generally limited to cases where plane strain prevails.
- The maximum crack size to be expected in service is $a_c = K_{Ic}^{\ 2} / \pi\beta^2\sigma^2$, where σ equals σ_{LT} or σ_{DM}, depending upon the inspectability level (see Section 1.3).

If stress-corrosion cracking is not expected at any crack size, the l-g stress, σ_{lg}, should be lower than $\sigma_{scc} = K_{Iscc} / \beta\sqrt{\pi a_c}$. With a_c given as above, it follows that complete prevention of stress corrosion extension of a fatigue crack requires selection of a material for which:

$$K_{Iscc} > \frac{\sigma_{\mathrm{lg}}}{\sigma_{LT}(or\,\sigma_{DM})} K_{Ic} \qquad (5.1.8)$$